PHYSICAL REVIEW LETTERS **129,** 183201 (2022)

Alignment Thresholds of Molecules

Joshua E. Szekely and Tamar Seideman[*]
Department of Chemistry, Northwestern University, Evanston, Illinois 60208, USA

(Received 30 June 2021; revised 23 August 2022; accepted 10 September 2022; published 24 October 2022)

Molecules have long been known to align in moderately intense, far off-resonance laser fields with a large variety of applications in physics and optics. We illustrate and describe the physical origin of a previously unexplored phenomenon in the adiabatic alignment dynamics of molecules, which is fundamentally interesting and also has an important practical implication. Specifically, the intensity dependence of the degree of adiabatic alignment exhibits a threshold behavior, below which molecules are isotropically distributed rotationally and above which the alignment rapidly reaches a plateau. Furthermore, we show that both the intensity and the temperature dependencies of the alignment of all linear molecules exhibit universal curves and derive analytical forms to describe these dependencies. Finally, we illustrate that the alignment threshold occurs very generally at a lower intensity than the off-resonance ionization threshold, a numerical observation that is readily illustrated analytically. The threshold behavior is attributed to a tunneling mechanism that rapidly switches off at the threshold intensity, where tunneling between the potential wells corresponding to the two orientations of the aligned molecules becomes impossible. The universal threshold behavior of molecular alignment is a simple phenomenon, but one that was not realized before and can be readily tested experimentally.

DOI: 10.1103/PhysRevLett.129.183201

Molecular alignment in moderately intense laser fields has been the focus of interest for over two decades, both for its fundamental value and for a large variety of applications, including enhancement of high harmonic generation [1,2], orbital imaging [3–7], investigation of orientation dependent ionization rates and patterns [8–13], control of laser filamentation [14–16], development of long range order in molecular assembly [17], control of electron and energy transfer [18], and more. The mathematical framework for describing molecular alignment by moderately intense laser fields in both adiabatic (long pulse) and nonadiabatic (short pulse duration compared to the rotational periods) was developed in the mid 1990s [19,20] and was since extended, generalized, and applied in a vast number of experimental and numerical publications [21–23]. Essentially all this work has been in the nonadiabatic domain.

Here, we illustrate a universal threshold behavior in adiabatic molecular alignment, below which molecules are isotropically distributed and above which the alignment rapidly saturates at its maximum value; see Fig. 1 (left panels). This phenomenon applies to all molecules (that can be aligned), regardless of their symmetry. The interest in the threshold phenomenon is due to both the interesting underlying fundamental physics involved (see below) and the implication to the generality of molecular alignment: while both nonresonant alignment and nonresonant ionization exhibit threshold behaviors, the alignment threshold is shown below to occur at a lower intensity (by location of the threshold we refer to the inflection point in the dependence of the alignment on the intensity). Because nonresonance ionization is the major competing process that upper bounds the degree of alignment (at least for small and mid-sized molecules) this finding implies that adiabatic alignment is much more broadly applicable than previously thought.

We show also that both the intensity and the temperature dependencies of linear alignment follow universal curves and derive simple analytical forms for these dependencies. These universal intensity and temperature dependencies imply that calculation of adiabatic alignment for an arbitrary molecule, in general a numerically costly task, can be made trivial. Finally, we discuss the physical significance of the universal intensity and temperature dependencies.

The total Hamiltonian is given as

$$\hat{H}_{\mathrm{tot}} = \hat{H}_{\mathrm{rot}} + \hat{H}_{\mathrm{ind}}[\vec{\varepsilon}(t)], \tag{1}$$

where $\hat{H}_{\mathrm{rot}}$ is the field-free rotational Hamiltonian (e.g., [22,24]). The field-matter interaction is the induced Hamiltonian, $\hat{H}_{\mathrm{ind}}$, written in the case of a nonresonant field as [22]

$$\hat{H}_{\mathrm{ind}} = -\frac{1}{4}\sum_{\rho,\rho'} \varepsilon_{\rho}\alpha_{\rho\rho'}\varepsilon^{*}_{\rho'}, \tag{2}$$

where $\rho, \rho' = \{x, y, z\}$ are the space-fixed Cartesian coordinates, we wrote the laser electric field as $\epsilon(t) = \frac{1}{2}\varepsilon(t)\exp(i\omega t) + \mathrm{c.c.}$, ω is the laser frequency, and $\alpha_{\rho\rho'}$ are components of the molecular polarizability tensor in the

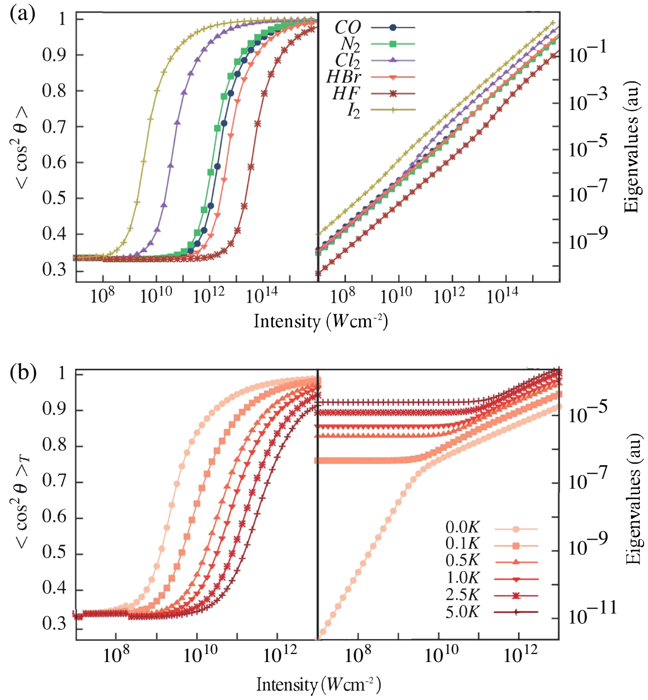

FIG. 1. Alignment thresholds and rotational energies (eigenvalues of the complete Hamiltonian) (a) for linear molecules (in this example, CO with $\Delta\alpha = 5.42$ Bohr^3, N$_2$ with $\Delta\alpha = 9.28$ Bohr^3, Cl$_2$ with $\Delta\alpha = 36.16$ Bohr^3, HBr with $\Delta\alpha = 11.2$ Bohr^3, HF with $\Delta\alpha = 3.27$ Bohr^3, and I$_2$ with $\Delta\alpha = 59.69$ Bohr^3), and (b) for symmetric top molecules (in this example, CHI$_3$ with $\Delta\alpha = 13.16$ Bohr^3). The absolute values of the eigenvalues are given to allow the logarithmic scale. Panel (a) shows that, when plotted as a function of a reduced interaction parameter $\varepsilon^2\Delta\alpha/B_e$, the alignment exhibits a universal curve. Panel (b) shows that temperature shifts the threshold intensity without altering its shape.

space-fixed frame. In the case considered here, the laser field is linearly polarized, $(\rho = \rho' = z)$, and Eq. (2) simplifies as

$$\hat{H}_{\text{ind}} = -\frac{\varepsilon^2(t)}{4}[\alpha^{ZX}\cos^2\theta + \alpha^{YX}\sin^2\theta\sin^2\chi], \quad (3)$$

where $\alpha^{kk'} = \alpha_{kk} - \alpha_{k'k'}$, α_{kk} are the diagonal components of the body-fixed polarizability, θ is the polar Euler angle between the space- and body-fixed z axes, and χ is the azimuthal Euler angle for rotation about the body-fixed z axis. In the case of linear and symmetric top molecules, $\hat{H}_{\text{ind}}$ simplifies further as

$$\hat{H}_{\text{ind}} = -\frac{1}{4}\varepsilon^2(t)\Delta\alpha\cos^2\theta, \quad (4)$$

where $\Delta\alpha$, the polarizability anisotropy, is the difference between the polarizability components parallel and perpendicular to the molecular axis.

The time-dependent Schrödinger equation subject to the Hamiltonian Eqs. (1), (3) (in the case of an asymmetric top) and Eqs. (1), (4) (in the case of a symmetric or linear top) is cast in the form of a set of coupled differential equations by expanding the wave function in a complete basis of rotational eigenstates appropriate to the molecular symmetry [25]. The degree of alignment of the molecular axis (the body-fixed z axis) to the field polarization axis (the space-fixed z axis) is quantified through the conventional expectation value $\langle\cos^2\theta\rangle(t) = \langle\Psi(t)|\cos^2\theta|\Psi(t)\rangle$, where $\Psi(t)$ is the time-dependent wave packet.

Figure 2 shows the maximum achieved alignment for N$_2$, starting from the rotational ground state, during a Gaussian pulse of varying duration. In the short pulse (impulse) limit, the alignment depends only on the fluence (rather than on the pulse shape, duration, and peak) and hence the intensity needed to generate a given alignment is inversely related to the pulse duration. Upon turn-on of the adiabatic mechanism, where the pulse duration exceeds the rotational period, a striking threshold behavior is observed. At higher intensities the alignment remains invariant to changes in the intensity.

Figure 1(a) (left panel) shows the average alignment, $\langle\cos^2\theta\rangle$, versus intensity for adiabatic alignment of several linear molecules, where the threshold behavior is evident. More interestingly, the alignment characteristics of all linear molecules follow a single universal curve when plotted versus the dimensionless interaction parameter $\varepsilon^2\Delta\alpha/B_e$, B_e being the rotational constant. Figure 1 (left panels) illustrates that a calculation of the adiabatic dynamics (a numerically costly task for either $k_BT \gg B_e$, k_B being the Boltzmann constant, or $\varepsilon^2\Delta\alpha \gg B_e$) can be avoided, as the alignment can be simply read off the universal plot. Furthermore, we show below that the alignment can be determined from an analytical universal equation. The right panels of Fig. 1 show the eigenvalues of the complete Hamiltonian (with the field-matter interaction included), determined by diagonalizing that Hamiltonian, as a function

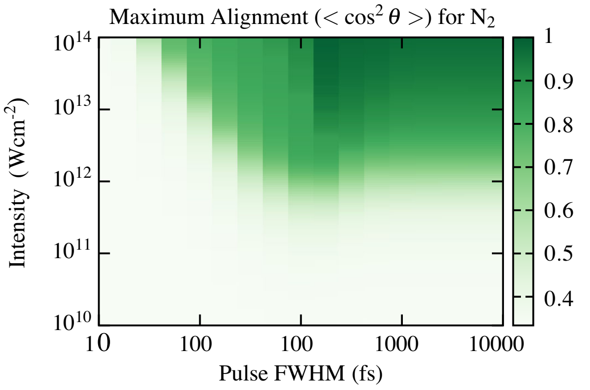

FIG. 2. Maximum alignment of N$_2$ during a Gaussian pulse. The plot includes only data acquired while the pulse is on, thus excluding a revival structure.

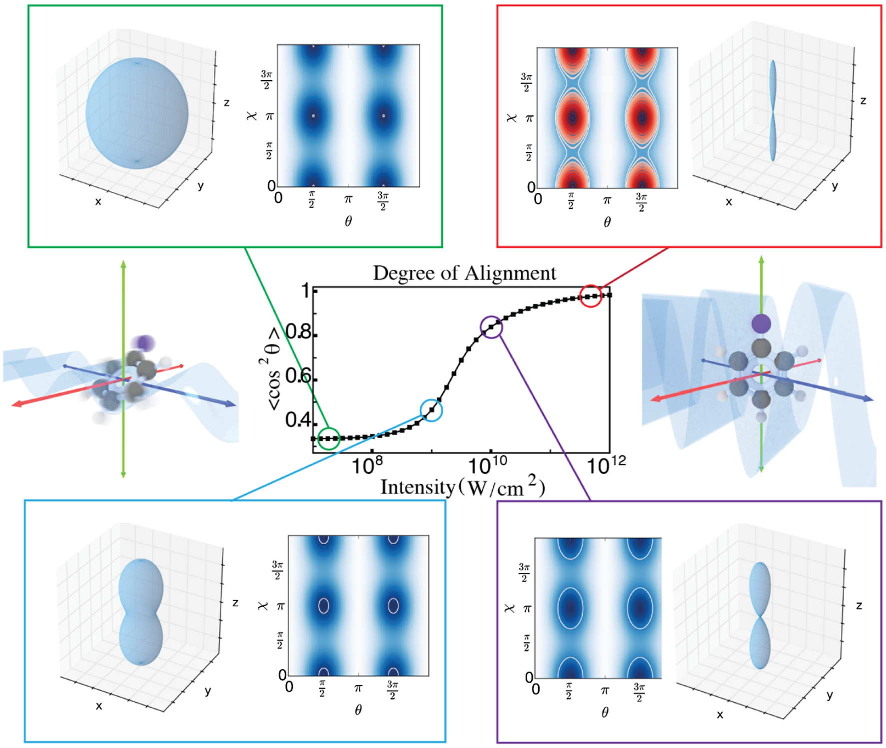

FIG. 3. Top and bottom: rotational eigenvalues (eigenvalues of the complete Hamiltonian) as contour maps and wave packets for an asymmetric top molecule (in this example, C_6H_5I). For the wave packet visualization, the rotation about the internal axis (χ) is set to zero. Center: the corresponding average alignment as a function of the intensity.

of the intensity. The significance of these eigenenergies is discussed below. Alignment thresholds are not unique to linear molecules. Figures 1(b) and 3 illustrate that they are exhibited for all molecular symmetries.

More usefully, the threshold behavior applies at all rotational temperatures, with the location of the threshold fully determined by the polarizability anisotropy and the reduced temperature $k_B T/B_e$. Figure 4, showing the location of the alignment threshold as a function of the (inverse of the) reduced temperature, illustrates that the temperature dependence of the alignment of all linear molecules falls on a single universal curve. The solid curve in Fig. 4 shows the result of fit of the data to the form $a(B_e/k_B T)^b + c$, where a, b, and c are fit parameters and the outcome $b = -1$ confirms the linearity in T. The linear dependence of the threshold intensity on the temperature is shown below to result from the dependence of the effective potential on the rotational states populated thermally before the laser pulse.

A complementary view of the role played by the rotational temperature of the initially prepared molecule is given in Fig. 1(b) (left panel), which illustrates that the rotational energy shifts the average alignment curve without modifying its shape. The threshold shift explains the extreme sensitivity of the alignment to the initial rotational temperature, illustrated in the experimental alignment literature [26–28].

The threshold behavior of $\langle\cos^2\theta\rangle$ results from a tunneling phenomenon. The laser-induced potential energy creates two potential minima corresponding to orientations of the molecule at $\theta = 0$ and π, which are separated by a potential barrier at $\pi/2$. At low intensities, where the induced potential is smaller than the rotational energy, the molecule is free to rotate, nearly unhindered by the barrier, and the alignment parameter is essentially constant at its isotropic value. As the intensity increases, the field-induced barrier grows above the rotational energy and the free rotation is replaced by tunneling. Further increase of the intensity fully localizes the probability density in the aligned configurations. The interplay between the laser-induced potential barrier and the rotational energy, which results in the threshold phenomenon, is illustrated for an asymmetric top in Fig. 3. Here, the induced potential energy, Eq. (3), is shown as a contour map with contours (white to red) indicating the values of the rotational eigenenergies of the complete Hamiltonian. The alignment is seen to exhibit a threshold at the intensity with which the interaction potential energy surpasses the eigenenergies.

To substantiate the tunneling mechanism and derive a closed-form expression for the alignment, we illustrate in the Supplemental Material [29] that the laser-induced potential energy barrier can be appropriately approximated by an Eckart potential [30], which admits an analytical solution for the tunneling coefficient. We show that the

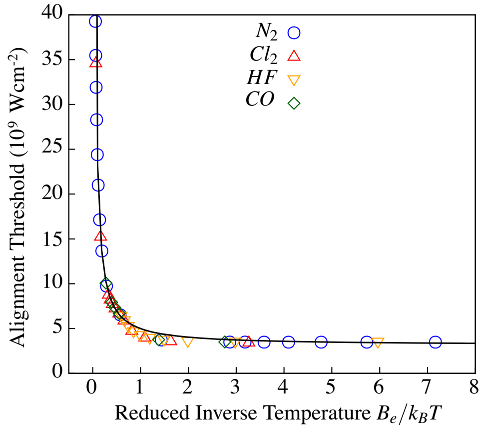

FIG. 4. A universal relation describing the adiabatic alignment threshold of all linear molecules versus the (inverse of the) reduced rotational temperature parameter k_bT/B_e.

alignment follows the tunneling curve, increasing from its isotropic value to close to unity as the tunneling probability decreases through a threshold to zero.

The linear behavior of the threshold versus the reduced rotational temperature results from the dependence of the effective potential on the competition between the interaction strength and the centrifugal barrier produced by the rotational levels that dominate the thermal distribution of the initial state. Specifically, Barrier $= [(-\Delta\alpha\varepsilon^2)/4B_e]\cos^2\theta + (M^2/\sin^2\theta)$, where M is the magnetic quantum number. Hence, for $T > 0$, the field-matter interaction $\propto \varepsilon^2$ must dominate over the centrifugal barrier $\propto M^2_{\max} = J^2_{i,\max}$, where $J_{i,\max}$ is the thermally populated angular momentum level dominating the initial Boltzmann distribution. For large J_i ($J_i \gg 1$), the rotational energy E_{J_i} is proportional to J_i^2/T, and thus the alignment threshold is expected to increase linearly with temperature, as observed.

The universal alignment threshold of molecules is a fascinating phenomenon but has in addition a ramification for future alignment experiments and for the generality of alignment as a tool. In the gas phase the degree of alignment is upper-bound by the onset of nonresonant ionization. The latter process is an intensively studied and well-understood problem, which exhibits a threshold dependence on the intensity, reflecting the onset of tunneling via the barrier formed when the laser electric field is added to the Coulomb field. The critical question is thus if the alignment threshold occurs at a substantially lower intensity than the ionization threshold and to what extent the answer to this question is general.

Qualitative considerations suggest that the answer is affirmative. Alignment relies on the polarizability tensor, which measures the ability of the field to distort the bound electron cloud. Tunnel ionization requires the field to bend the Coulomb potential sufficiently for the electron to tunnel out. This suggests that the alignment threshold substantially precedes the tunnel ionization threshold. Quantitative calculations and measurements support this qualitative anticipation, as illustrated in Fig. 5.

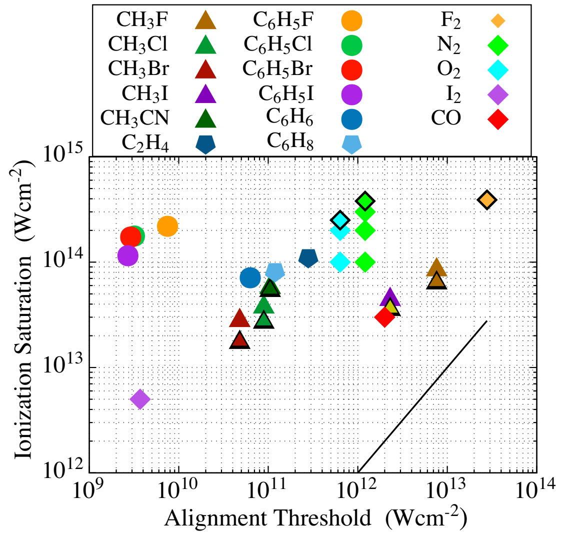

FIG. 5. Ionization saturation intensities plotted against alignment thresholds for a variety of molecules. All values lie an order of magnitude or more above the black line (which corresponds to equal ordinate and abscissa), illustrating that at nonresonant frequencies, alignment takes place at an order of magnitude or more lower intensity than ionization for all explored systems. The black outlined points show numerical results obtained within the Perelomov, Popov and Terent'ev theory for the methyl halides and within the strong field approximation for the other molecules. The remaining results are experimental. The methyl halides are found in Ref. [31], phenyl halides and C_6H_5CN in Ref. [32], unsubstituted hydrocarbons in [33], F_2 [34], N_2 [34–37], O_2 [34,37,38], I_2 [39], and CO [37].

Here, ionization saturation intensities for various molecules are plotted against their alignment thresholds. For all molecules we have considered, the ground state alignment threshold is observed at an intensity over an order of magnitude smaller than the ionization threshold. We note that the ionization experiments in Fig. 5 correspond to pulse durations ranging from femtoseconds to nanoseconds, where experiments in iodine-containing aromatic compounds [26] used adiabatic pulses, and for nitrogen ionization experimental results are available over a wide range of pulse durations [34–37]. For the short pulse case, the ionization thresholds in Fig. 5 are likely to overestimate the ionization thresholds with pulse durations exceeding the rotational period, but given the large disparity between the ionization and alignment threshold intensities seen in Fig. 5, the alignment threshold intensity is expected to remain well below the relevant, long-pulse ionization threshold.

Summarizing, we illustrated a fascinating phenomenon in the adiabatic alignment dynamics of molecules, namely, a threshold dependence of the alignment on the laser intensity, which applies to all molecules. Both the alignment intensity dependence and the dependence of the threshold intensity on the rotational temperature are universal. Further, both dependencies are described by simple analytical expressions that could replace heavy numerical calculations. Underlying the threshold effect is a barrier tunneling mechanism. In addition to its fundamental interest, the threshold phenomenon carries an implication for the value of alignment as a general tool, as we show that the alignment threshold precedes that of the ionization as the intensity increases at nonresonant frequencies. This generality will be particularly important as alignment is extended to large polyatomic systems.

We thank the Department of Energy (Award No. DE-FG02-04ER15612/0013) for support of the research leading to this manuscript.

---

[*]Corresponding author.
t-seideman@northwestern.edu

[1] J. Heslar, J. Carrera, D. Telnov, and S.-I. Chu, High-order harmonic generation of heteronuclear diatomic molecules in intense ultrashort laser fields: An all electron TDDFT study, Int. J. Quantum Chem. **107**, 3159 (2007).

[2] C. Zhang, J. Yao, F. a. Umran, J. Ni, B. Zeng, G. Li, and D. Lin, Enhanced narrow-bandwidth emission during high-order harmonic generation from aligned molecules, Opt. Express **21**, 3259 (2013).

[3] J. Itatani, J. Levesque, D. Zeidler, H. Niikura, H. Pépin, J. C. Kieffer, P. B. Corkum, and D. M. Villeneuve, Tomographic imaging of molecular orbitals, Nature (London) **432**, 867 (2004).

[4] D. Dimitrovski, M. Abu-Samha, L. B. Madsen, F. Filsinger, G. Meijer, J. Küpper, L. Holmegaard, L. Kalhøj, J. H. Nielsen, and H. Stapelfeldt, Ionization of oriented carbonyl sulfide molecules by intense circularly polarized laser pulses, Phys. Rev. A **83**, 023405 (2011).

[5] C. Vozzi, M. Negro, F. Calegari, G. Sansone, M. Nisoli, S. De Silvestri, and S. Stagira, Generalized molecular orbital tomography, Nat. Phys. **7**, 822 (2011).

[6] J. B. Bertrand, Linked attosecond phase interferometry for molecular frame measurements, Nat. Phys. **9**, 174 (2013).

[7] J. Tross, X. Ren, V. Makhija, S. Mondal, V. Kumarappan, and C. A. Trallero-Herrero, N_2 HOMO-1 orbital cross section revealed through high-order-harmonic generation, Phys. Rev. A **95**, 033419 (2017).

[8] M. Schmidt, S. Dobosz, P. Meynadier, P. D'Oliveira, D. Normand, E. Charron, and A. Suzor-Weiner, Fragment-emission patterns from the Coulomb explosion of diatomic molecules in intense laser fields, Phys. Rev. A **60**, 4706 (1999).

[9] H. Li, D. Ray, S. De, I. Znakovskaya, W. Cao, G. Laurent, Z. Wang, M. F. Kling, a. T. Le, and C. L. Cocke, Orientation dependence of the ionization of CO and NO in an intense femtosecond two-color laser field, Phys. Rev. A **84**, 043429 (2011).

[10] S.-F. Zhao, J. Xu, C. Jin, A.-T. Le, and C. D. Lin, Effect of orbital symmetry on the orientation dependence of strong field tunnelling ionization of nonlinear polyatomic molecules, J. Phys. B **44**, 035601 (2011).

[11] J. L. Hansen, L. Holmegaard, J. H. Nielsen, H. Stapelfeldt, D. Dimitrovski, and L. B. Madsen, Orientation-dependent ionization yields from strong-field ionization of fixed-in-space linear and asymmetric top molecules, J. Phys. B **45**, 015101 (2012).

[12] J. Wu, X. Gong, M. Kunitski, F. K. Amankona-Diawuo, L. P. H. Schmidt, T. Jahnke, a. Czasch, T. Seideman, and R. Dörner, Strong Field Multiple Ionization as a Route to Electron Dynamics in a van der Waals Cluster, Phys. Rev. Lett. **111**, 083003 (2013).

[13] P. Sandor, A. Sissay, F. Mauger, M. W. Gordon, T. T. Gorman, T. D. Scarborough, M. B. Gaarde, K. Lopata, K. J. Schafer, and R. R. Jones, Angle-dependent strong-field ionization of halomethanes, J. Chem. Phys. **151**, 194308 (2019).

[14] J. P. Palastro, T. M. Antonsen, and H. M. Milchberg, Compression, spectral broadening, and collimation in multiple, femtosecond pulse filamentation in atmosphere, Phys. Rev. A **86**, 033834 (2012).

[15] P. Lu, J. Wu, and H. Zeng, Manipulation of plasma grating by impulsive molecular alignment, Appl. Phys. Lett. **103**, 221113 (2013).

[16] N. Berti, P. Bejot, J. P. Wolf, and O. Faucher, Molecular alignment and filamentation: Comparison between weak and strong field models, Phys. Rev. A **90**, 053851 (2014).

[17] I. Nevo, S. Kapishnikov, A. Birman, M. Dong, S. R. Cohen, K. Kjaer, F. Besenbacher, H. Stapelfeldt, T. Seideman, and L. Leiserowitz, Laser-induced aligned self-assembly on water surfaces, J. Chem. Phys. **130**, 144704 (2009).

[18] M. G. Reuter, M. Sukharev, and T. Seideman, Laser Field Alignment of Organic Molecules on Semiconductor Surfaces: Toward Ultrafast Molecular Switches, Phys. Rev. Lett. **101**, 208303 (2008).

[19] T. Seideman, Rotational excitation and molecular alignment in intense laser fields, J. Chem. Phys. **103**, 7887 (1995).

[20] B. Friedrich and D. Herschbach, Alignment and Trapping of Molecules in Intense Laser Fields, Phys. Rev. Lett. **74**, 4623 (1995).

[21] H. Stapelfeldt and T. Seideman, Colloquium: Aligning molecules with strong laser pulses, Rev. Mod. Phys. **75**, 543 (2003).

[22] N. Moiseyev and T. Seideman, Alignment of molecules by lasers: Derivation of the Hamiltonian within the (t, t') formalism, J. Phys. B **39**, L211 (2006).

[23] Y. Ohshima and H. Hasegawa, Coherent rotational excitation by intense nonresonant laser fields, Int. Rev. Phys. Chem. **29**, 619 (2010).

[24] R. N. Zare, *Angular Momentum: Understanding Spatial Aspects in Chemistry and Physics* (Wiley, New York, 1988), p. 349.

[25] These are spherical harmonics for linear molecules or normalized Wigner D matrices for symmetric tops. Linear molecules that possess electronic angular momentum behave like symmetric tops. In the case of asymmetric top molecules, although it is possible to expand the wave function in a basis of asymmetric top eigenstates, it is often convenient to use normalized Wigner matrices and include

the field-free asymmetric top coupling together with the radiative coupling.

[26] V. Kumarappan, C. Z. Bisgaard, S. S. Viftrup, L. Holmegaard, and H. Stapelfeldt, Role of rotational temperature in adiabatic molecular alignment, J. Chem. Phys. **125**, 194309 (2006).

[27] V. Kumarappan, S. S. Viftrup, L. Holmegaard, C. Z. Bisgaard, and H. Stapelfeldt, Aligning molecules with long or short laser pulses, Phys. Scr. **76**, C63 (2007).

[28] S. Trippel, T. G. Mullins, N. L. Muller, J. S. Kienitz, K. Dlugolecki, and J. Kupper, Strongly aligned and oriented molecular samples at a khz repetition rate, Mol. Phys. **111**, 1738 (2013).

[29] See Supplemental Material at http://link.aps.org/supplemental/10.1103/PhysRevLett.129.183201 for derivation of an analytical expression for the adiabatic alignment vs intensity.

[30] C. Eckart, The pennetration of a potenital barrier by electrons, Phys. Rev. **35**, 1303 (1930).

[31] M. Tanaka, M. Murakami, T. Yatsuhashi, and N. Nakashima, Atomiclike ionization and fragmentation of a series of CH3-X (X: H, F, Cl, Br, I, and CN) by an intense femtosecond laser, J. Chem. Phys. **127**, 104314 (2007).

[32] T. D. Scarborough, J. Strohaber, D. B. Foote, C. J. McAcy, and C. J. G. J. Uiterwaal, Ultrafast REMPI in benzene and the monohalobenzenes without the focal volume effect, Phys. Chem. Chem. Phys. **13**, 13783 (2011).

[33] S. M. Hankin, D. M. Villeneuve, P. B. Corkum, and D. M. Rayner, Intense-field laser ionization rates in atoms and molecules, Phys. Rev. A **64**, 013405 (2001).

[34] V. I. Usachenko, P. E. Pyak, and V. V. Kim, Comparative study of strong-field ionization in laser-irradiated F_2 and other diatomic molecules: Density-functional-theory-based molecular strong-field approximation, Phys. Rev. A **79**, 023415 (2009).

[35] J. H. Posthumus, The dynamics of small molecules in intense laser fields, Rep. Prog. Phys. **67**, 623 (2004).

[36] A. I. Pegarkov, E. Charron, and A. Suzor-Weiner, Nonlinear single and double ionization of molecules by strong laser pulses, J. Phys. B **32**, L363 (1999).

[37] T. D. G. Walsh, F. a. Ilkov, J. E. Decker, and S. L. Chin, The tunnel ionization of atoms, diatomic and triatomic molecules using intense 10.6 mu m radiation, J. Phys. B **27**, 3767 (1994).

[38] M. J. DeWitt, E. Wells, and R. R. Jones, Ratiometric Comparison of Intense Field Ionization of Atoms and Diatomic Molecules, Phys. Rev. Lett. **87**, 153001 (2001).

[39] D. Normand and M. Schmidt, Multiple ionization of atomic and molecular iodine in strong laser fields, Phys. Rev. A **53**, R1958 (1996).